Int. J. Appl. Math. Comput. Sci., 2022, Vol. 32, No. 4, 619–634
DOI: 10.34768/amcs-2022-0043

TOWARDS A HEALTH–AWARE FAULT TOLERANT CONTROL OF COMPLEX SYSTEMS: A VEHICLE FLEET CASE

BOGDAN LIPIEC [a,*], MARCIN MRUGALSKI [a], MARCIN WITCZAK [a], RALF STETTER [b,c]

[a]Institute of Control and Computation Engineering
University of Zielona Góra
ul. Szafrana 2, 65-516 Zielona Góra, Poland
e-mail: {b.lipiec,m.mrugalski,m.witczak}@issi.uz.zgora.pl

[b]Faculty of Mechanical Engineering
University of Applied Sciences Ravensburg–Weingarten
Doggenriedstraße, 88250, Weingarten, Germany
e-mail: stetter@hs-weingarten.de

[c]Steinbeis Transfer Center for Automotive Systems
Raueneggstraße 29/1, 88212, Ravensburg, Germany

The paper deals with the problem of health-aware fault-tolerant control of a vehicle fleet. In particular, the development process starts with providing the description of the process along with a suitable Internet-of-Things platform, which enables appropriate communication within the vehicle fleet. It also indicates the transportation tasks to the designated drivers and makes it possible to measure their realization times. The second stage pertains to the description of the analytical model of the transportation system, which is obtained with the max-plus algebra. Since the vehicle fleet is composed of heavy duty machines, it is crucial to monitor and analyze the degradation of their selected mechanical components. In particular, the components considered are ball bearings, which are employed in almost every mechanical transportation system. Thus, a fuzzy logic Takagi–Sugeno approach capable of assessing their time-to-failure is proposed. This information is utilized in the last stage, which boils down to health-aware and fault-tolerant control of the vehicle fleet. In particular, it aims at balancing the exploitation of the vehicles in such a way as to maximize they average time-to-failure. Moreover, the fault-tolerance is attained by balancing the use of particular vehicles in such a way as to minimize the effect of possible transportation delays within the system. Finally, the effectiveness of the proposed approach is validated using selected simulation scenarios involving vehicle-based transportation tasks.

Keywords: FTCD, modeling bearings degradation, remaining useful life prediction, health-aware fault tolerant control, Takagi–Sugeno model.

1. Introduction

There is a belief in society that mechanical systems, unlike electronic ones, are burdened with a higher failure rate. This view may in part be justified because mechanical systems largely consist of components that slowly but inevitably degrade over time. This degradation results from the gradual deterioration of the physical or chemical properties of the component due to prolonged use. Such gradual deterioration of component parameters leads to faults that can lead to irreversible failures of the entire system.

Among the mechanical components that fail most frequently are the bearings (Liu and Zhang, 2020; Duan *et al.*, 2018; Wei *et al.*, 2019). This is due to the fact that they are subjected to a high and long-term mechanical stress. If proper operation and/or service conditions are not ensured, their quality parameters deteriorate rapidly.

Bearings have numerous applications in many systems, such as vehicles, electric and mechanical machines and wind turbines (AlShorman *et al.*, 2020; Wei

*Corresponding author

et al., 2019; Duan *et al*., 2018). Due to the numerous applications of bearings, any research aimed at extending their service life is of a great economic importance. In the literature, there are many fault diagnostics (FD) (Witczak, 2014; Witczak *et al.*, 2020c; Pazera *et al*., 2020; Mrugalski and Korbicz, 2007) methods based on, for example, vibroacoustic methods (AlShorman *et al*., 2021), artificial intelligence based methods (Nath *et al*., 2021), observer-based approaches (Gao and Liu, 2021), which are aimed at fault detection of bearings and replacing them with new ones at the time of pre-emergency or after a failure.

However, this paper proposed a completely different and holistic approach leading to the extended service life of bearing systems. This approach assumes that we can gradually use individual elements included in the system, taking into account the degree of their degradation. For example, if we have at our disposal a group of vehicles characterized by various degrees of bearing degradation, then having this knowledge, we can use these vehicles to varying degrees in order to ensure the longest possible level of operation of all vehicles. In other words, if we know that one of the vehicles has heavily worn bearings, it will be less frequently used for the transport task. However, other factors should also be mentioned, such as increased energy consumption, speed limits, emergency mechanical blockage. By using a less frequently damaged vehicle, it is possible to minimize their impact on the system and the possibility of failure. The above approach is also known as health-aware fault tolerant control (H-A FTC) (Lipiec *et al*., 2021; Jain and Yamé, 2020; Salazar *et al*., 2020).

An effective H–A FTC system should have functionalities capable of modeling system degradation, system diagnostics, remaining useful life (RUL) prediction (Zhou *et al*., 2019), and robust FTC (Witczak, 2014; Hamdi *et al*., 2021). The modeling of the degradation process is usually done using artificial neural networks (Chen *et al*., 2020; Wang *et al*., 2018; Li *et al*., 2018), life expectancy models (Chudnovsky, 2012), knowledge based models (Do *et al*., 2018) and physical models (Sun *et al*., 2019). One of the basic disadvantages of the above methods is that they do not have a mathematical description of the uncertainty of the prediction process, which make them impossible to use in H-A FTC systems.

In order to overcome this disadvantage, in this article a method that combines exponential models and the fuzzy logic framework was developed. Such a method enables not only modeling qualitative changes in vehicle bearings, but also carrying out fault detection. Moreover, this work proposes the RUL prediction method. The purpose of this method is to determine the trajectory of the deteriorating state of the system from the moment of fault detection to its complete failure using the time-to-failure (TTF) indicator (Witczak, 2014). The concept of the developed data-driven based remaining useful life prediction method is based on the application of a group of Takagi–Sugeno (T–S) models (Xie *et al*., 2021). The proposed method enables the development of a comprehensive method of controlling a group of vehicles, taking into account the degradation condition of their bearings, the occurrence of potential faults in the system, transport delays, etc. Moreover, a new health-aware based cost function, which takes into account predictions concerning the current operational ability of wheel loaders bearings is proposed. The proposed H-A FTC scheme was validated on the theoretical model of the transport task of the rock aggregate transported with the use of a group of wheel loaders (WLs), where the degradation models for their bearings were built based on the real data from the PRONOSTIA test platform (Nectoux *et al*., 2012). A wheel loader is usually used to build roads, prepare the job site, dig and carry heavy loads, or move materials.

The paper is organized as follows. Section 2 presents the motivation to undertake research and describes the system under consideration. Section 3 presents the basic system constraints that should be taken into account when designing the H-A FTC method. Section 5 presents a new fuzzy logic based approach to modeling the bearing degradation process. Section 6 shows the new RUL prediction method. Section 7 presents an algorithm for H-A FTC of multiple wheel loaders. Section 8 shows the results of the efficiency evaluation of the proposed H-A FTC strategy and Section 9 concludes the paper.

2. System description

The process considered is carried out in a sample plant producing aggregates used for road hardening. The plant produces aggregate fractions (from 2 mm to 8 mm). It is used while hardening roads under construction. Five loading stations, where bucket trucks arrive, are operated by five wheel loaders. Five aggregate storage places are continuously refilled by conveyor belts that are linked to aggregate production.

Having a layout of the loading area (see Fig. 1), suitable communication tools have to be implemented. This solution enables tracking the driver's performance and provides information about current tasks on time reliably and safely.

To solve the so formulated problem, the new IoT infrastructure KIS.ME (Keep.It.Simple Manage.Everything) is proposed. This infrastructure provides two components:

KIS.BOX: a button box equipped with a WiFi interface,

KIS.LIGHT: a signal LED equipped with a WiFi interface.

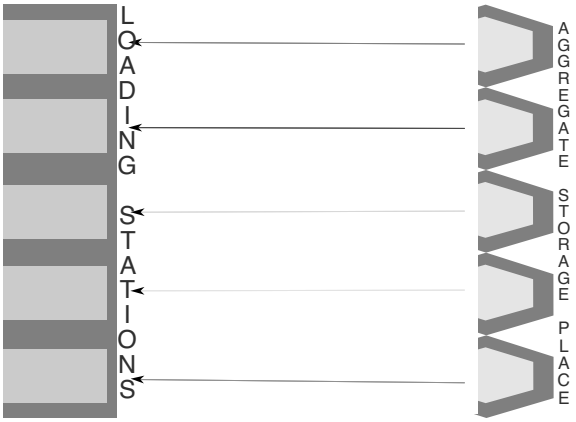

Fig. 1. Sample loading area.

The KIS.LIGHT buttons and KIS.BOX can light in several specified colors. The advantage under discussion can be efficiently used for human-machine communication within the loading area.

The structure of proposed solution is very intuitive and considers two main points:

- **KIS.LIGHT**s stand at restricted loading stations, where dump trucks are loaded by wheel loaders,
- **KIS.BOX**es are installed on a wheel loader performing loading tasks.

KIS.Manager allows virtualizing all KIS.BOXes and KIS.LIGHTs. The KIS.Manager enables the visualization of the digital twin of all KIS.Lights and KIS.BOXes in the loading space. What is more, using KIS.Manager, it is possible to represent the states of buttons while the visualization of movements is not implemented. Such functionalities simplify the device representations. To solve this problem, the device position identification is based on the parameters provided by the manufacturing execution system (MES)

$$\mathbb{N}(k) = \{D(k), L(k), M(k)\}, \tag{1}$$

where

- k is the loading event counter, i.e., $k = 0, 1, \ldots,$
- $D(k)$ is the identifier of an aggregate storage place,
- $L(k)$ is the identifier of a loading station,
- $M(k)$ is the k-th mass of ordered aggregate (in kg).

We assume that the distance between the loading stations and the aggregate storage places is the same for all routes. Each station is assigned to a specific fraction that can be loaded there. The main factor that distinguishes the tasks is the number of tons that must be loaded into the dump truck. In the considered aggregate production plant,

Algorithm 1. KIS.ME procedure.

S_1 : The loading station KIS.LIGHT $L(k)$ lights with a green color. A new task has been assigned.

S_2 : The selected wheel loader KIS.BOX ring illuminates with a green colour.

S_3 : The WL driver pushes first the KIS.BOX button. It starts flashing in green. Second KIS.BOX button color indicates the mass of a loading aggregate (see Table 1). The awaiting time b_i is saved. The operator starts transportation event $\mathbb{L}(k)$.

S_4 : When the loading task is completed, the WL driver pushes first the KIS.BOX button. Its ring becomes black. The transportation time c_i is saved.

the loading capacity of the loader bucket is 2 tons. For the purpose of further deliberations, the work schedule on a given horizon must be assumed, which shapes the desired transportation plan:

$$\mathbb{Q} = \{\mathbb{N}(0), \mathbb{N}(1), \ldots, \mathbb{N}(n_E)\}, \tag{2}$$

where n_E is the number of loading tasks while the other variables being used are as follows:

- n_T stands for the number of all loading stations,
- n_E signifies the number of all wheel loaders,
- $u(k)$ is the unknown loading start time of the k-th loading task from $D(k)$ towards $L(k)$, which has to be determined,
- $v_i(k)$ (for $i = 1, \ldots, n_E$) is a two-valued decision variable indicating which wheel loader undertakes transportation event $\mathbb{N}(k)$;
- $z_i(k)$ is the time when the i-th wheel loader ($i = 1, \ldots, n_v$) is ready to perform transportation event $\mathbb{N}(k)$,
- $v_{n_v+1}(k)$ is the time of realizing the k-th task.

The KIS.ME IoT platform is applied to determine a loader driver performance model. A step-by-step procedure is described as Algorithm 1.

The sample signalization presented in Fig. 2 shows the situation, when the task is assigned to the first station and 13 000 kg should be loaded.

3. Health-aware fault-tolerant control

In order to develop an H-A FTC strategy that takes into account the remaining useful life of vehicles bearings,

Table 1. Color description of loaded mass.

Color	Loading mass (kg)
magenta	6 500
blue	10 000
turquoise	13 500
green	17 000
red	21 500
yellow	28 000
white	31 500

Fig. 2. Sample task signalization.

several constraints describing the behavior of the whole system presented in Section 2 should be defined.

Wheel loaders movement restrictions. The k-th vehicle should leave $T(k)$ before the l-th ($l > k$) aggregate package will be delivered:

$$\text{IF } l > k \text{ and } T(k) = T(l) \text{ THEN } u(k) \leq u(l) + \alpha(j), \tag{3}$$

where $\alpha(j) > 0$ denotes the unknown variable time between receiving the k-th and l-th loads. This limitation is to prevent a situation where two different loads are transported from the same loading bay at the same time, i.e., $u(k) = u(l)$. Nevertheless, it is obvious that time $\alpha(l)$ should be as short as possible. Moreover, it should be also assumed that $j = 1 \ldots, n_\alpha$, $n_\alpha < n_E$. In order to meet this condition, an expected transportation plan $\mathbb{P}$ given by (2) has to be obtained.

Scheduling restriction. This restriction means that each of the n_E starting times for loading a rock aggregate by the wheel loader is limited:

$$u(k) \leq u_E, \tag{4}$$

where $u_E > 0$ s the maximum allowable start time for the transportation of all n_E rock aggregate loads.

Transportation restriction. The operating time of the i-th wheel loader transporting the k-th load of rock aggregate is related to its degree of degradation:

$$b_i(k) = \max\left(e, b(k) + v_i(k)\right), \tag{5}$$

$$c_i(k) = \max\left(e, c(k) + v_i(k)\right). \tag{6}$$

As can be seen, when the i-th wheel loader is not carrying the k-th load of rock aggregate then $v_i(k) = \varepsilon = -\infty$, which means that $b_i(k) = c_i(k) = \max(e, \varepsilon) = \max(0, \varepsilon) = 0$.

Concurrency restriction. This condition defines the obvious situation that the k-th load of rock aggregate can be transported only by one, the j-th wheel loader:

$$v_j(k) = e \quad \Leftrightarrow \quad v_i(k) = \varepsilon, \quad \forall i \neq j. \tag{7}$$

All the above-defined restrictions make it possible to develop a control strategy that takes into account the state of degradation of the wheel loader bearings. Indeed, the problem lies in the determination of the sequence of pairs:

$$(u(k), v_i(k)), \quad k = 0, \ldots, n_E - 1, \tag{8}$$

resulting in the k-th rock aggregate load transportation start time $u(k)$ along with $v_i(k)$, the i-th wheel loader doing this activity.

Assume the following cost functions associated with:

- minimizing

$$J_u = -\sum_{k=0}^{n_E-1} u(k), \tag{9}$$

  which means determining the maximum possible average time of loading rock aggregate;

- minimizing the time of picking up of rocks from a given loading bay,

$$J_\alpha = \sum_{j=1}^{n_\alpha} \alpha(j); \tag{10}$$

- minimizing

$$J_H = -\sum_{k=0}^{n_E-1} \sum_{i=1}^{n_E} (\bar{t}_i - b_i(k) - c_i(k)), \tag{11}$$

  where $\bar{t}_i$ is the expected time-to-failure of the i-th loader.

Note that exact values of $\bar{t}_i$ are impossible to attain. However, they can be efficiently estimated with the approach proposed in Section 6. The cost functions (9)–(11) define various goals which together can be achieved by minimizing the following compound criterion:

$$J = \gamma_1 J_u + \gamma_2 J_\alpha + \gamma_3 J_H, \tag{12}$$

$$\gamma_1 + \gamma_2 + \gamma_3 = 1, \quad \gamma_i \geq 0, \quad i = 1, 2, 3, \tag{13}$$

where coefficient γ_i weighs the role of a current restriction and appropriate selection of these values leads to a desired system behavior.

The knowledge about (12) and constraints (3)–(7) allows proposing a method for modeling and control of multiple wheel loaders which are similar to that proposed for the fleet of forklifts by Witczak *et al.* (2020a).

4. Health-aware control of multiple wheel loaders

In this section a model for predicting the future behavior of multiple wheel loaders is proposed. Such a model is based on the max-plus algebra (M-PA) scheme (Majdzik *et al.*, 2016; 2021; Seybold *et al.*, 2015; De Schutter and Van den Boom, 2001; Van Den Boom and De Schutter, 2006; Witczak *et al.*, 2020b). Unlike the well-known M-PA models, the property of the method developed by Witczak *et al.* (2020a) is that it allows handling both system synchronization and concurrency. To obtain such a property, the re-called model uses a set of decision variables $\{v_i(k)\}_{k=1}^{N_p}$ for an assumed prediction horizon $N_p < n_E$. It is worth emphasizing that the M-PA structure ($\mathbb{R}_{\max}$, $\oplus$,$\otimes$) involves the following properties and operations: $\mathbb{R}_{\max} \triangleq \mathbb{R} \cup \{-\infty\}$, for all $x, y \in \mathbb{R}_{\max}$, where $x \oplus y = \max(x, y)$, for all $x, x \in \mathbb{R}_{\max}$ and $x \otimes x = x + y$ whereas $\mathbb{R}$ denotes the field of real numbers. The above-described operations can be represented in matrix form (Butkovic, 2010).

Based on the assumed definitions, the behavior of n_E wheel loaders can be written as

$$z(k) = A(v(k), k) \otimes z(k-1) \oplus B(v(k), k) \otimes u(k), \tag{14}$$

where

- $z(k) = [z_1(k), z_2(k), \ldots, z_{n_E}(k), z_{n_E+1}(k)]^T$,
- $v(k) = [v_1(k), \ldots, v_{n_E}(k)]^T$,
- $\boldsymbol{A}(\cdot,\cdot) \in \mathbb{R}_{\max}^{n_E+1 \times n_E+1}$,
- $z(k)$ is the transition matrix,
- $\boldsymbol{B}(\cdot,\cdot) \in \mathbb{R}_{\max}^{n_v+1}$ is the control matrix.

Moreover, the transformation and control matrices are defined by (15).

The multiple wheel loader health-aware control strategy relies on the selection of the input sequence $u(k), \ldots, u(k + N_p - 1)$ on the assumed horizon $k, \ldots, k + N_p - 1$ in order to minimize cost function J defined by relation (12).

According to the method described by Witczak *et al.* (2020a), the prediction vector $\tilde{w}(k) = [w(k)^T, w(k+1)^T, \ldots, w(k+N_p-1)^T]^T$ has to be defined. Then the recursive use of the expression (14) leads to

$$\tilde{z}(k) = \boldsymbol{M}(\tilde{v}(k)) \otimes \tilde{z}(k-1) \oplus \boldsymbol{H}(\tilde{v}(k)) \otimes \tilde{u}(k), \tag{16}$$

where $\boldsymbol{M}(\tilde{v}(k))$ and $\boldsymbol{H}(\tilde{v}(k))$ are calculated by a chain of recursive substitutions (Witczak *et al.*, 2020a).

After the above transformations, the health-aware control task relies on solving the following optimization problem for each k

$$\left(\tilde{u}(k)^*, \tilde{v}(k)^*, \tilde{\alpha(k)}^*\right) = \arg \min_{\tilde{u}(k), \tilde{v}(k), \tilde{\alpha(k)}} J, \tag{17}$$

subject to the constraints (3)–(7).

The results obtained in this section form a basis for the development of a new H-A FTC method which can be applied to a fleet of wheel loaders.

5. Fuzzy logic approach to modelling the degradation process

The exponential models enable us to create tools for modeling the degradation process of many common components, which are used in industry (Zhang *et al.*, 2018; Anis, 2018), including the 2021 PHM Data Challenge (Singleton *et al.*, 2015; Sutrisno *et al.*, 2012). The main part of this challenge is testing the platform PRONOSTIA. The main objective of this section is to combine together exponential modeling with historical data collected from the ball bearing the same type. For that reason a fuzzy logic framework is presented in this section.

The following structure of the exponential degradation model should be mentioned (see, e.g., the works of Li *et al.* (2015) or Gebraeel *et al.* (2005)) and the references therein):

$$x_k = \phi + \theta_k \exp\left(\beta_k t_k + \sigma_k \mathcal{B}(t_k) - \frac{\sigma_k^2}{2} t_k\right), \tag{18}$$

where

- k represents the number of the sample,
- x_k is the degradation parameter being modeled (e.g., a vibration),
- ϕ is a constant known as the minimum bound of the degradation parameter,
- β, σ and θ are unknown parameters, which are responsible for shaping the behavior of the exponential model,
- t_k is a time at a given sample k,
- $\sigma\mathcal{B}(t_k)$ denotes a Brownian motion obeying a normal distribution $\mathcal{N}(0, \sigma^2 t_k)$.

The model (18) yields a logarithmic transform of the traditional form

$$\begin{aligned} m_k &= \ln(x_k - \phi) \\ &= \ln(\theta_k) + \left(\beta_k - \frac{\sigma_k^2}{2}\right) t_k + \sigma_k \mathcal{B}(t_k), \end{aligned} \tag{19}$$

$$A(v(k),k)=\begin{bmatrix} b_1(k-1)+c_1(k-1) & \varepsilon & \dots & \varepsilon \\ \varepsilon & b_2(k-1)+c_2(k-1) & \dots & \varepsilon \\ \vdots & \vdots & \ddots & \vdots \\ b_1(k-1)+c_1(k-1)+c_1(k)+v_1(k) & b_2(k-1)+c_2(k-1)+c_2(k)+v_2(k) & \dots & h(k) \end{bmatrix},$$
$$B(v(k),k)=[v_1(k),v_2(k),\dots,v_{n_v}(k),\max(c_1(k)+v_1(k),\dots,c_{n_v}(k)+v_{n_v}(k))]^T. \tag{15}$$

which is transformed into a compact regressor-like form

$$m_k = r_k^T p_k, \tag{20}$$

with

$$r_k=[1,t_k]^T, \quad p_k=\left[\ln(\theta),\beta-\frac{\sigma^2}{2}\right]^T. \tag{21}$$

where $r_k \in \mathbb{R}^2$ represents the regressor vector and $p_k \in \mathbb{R}^2$ means a time-varying parameter vector.

5.1. Fuzzy logic in the bearing degradation processes representation. The development of a method for remaining useful life estimation of bearings in HV requires knowledge of a model of the bearing degradation process. This model can be created in the identification process on the basis of a set of measurement data from many bearings with different degradation rates. The method used to model the bearing degradation process should be highly accurate despite the presence of measurement noise or uncertainties. Moreover, the method should have computational simplicity allowing its application in real time. The tool that meets the above requirements is fuzzy logic.

Let us assume that the model (20) can be simplified by accepting that $\phi = 0$. Gebraeel *et al*. (2005) and Li *et al*. (2015) showed that ϕ is known or it can be obtained from x_k. Thus, omitting ϕ from the model (20) does not deteriorate the accuracy of the degradation model. The above assumption yields $m_k = x_k$.

The degradation signal z_k can be constrained just like the variable m_k:

$$\underline{m} \le m_k \le \bar{m}, \tag{22}$$

which, when outside the limit values, is considered to be the minimum symptom of degradation. In other words, $\bar{m} > 0$ represents the maximum allowable degradation level. Of course, when m_k value remains within the range (22), we assume that the bearing is undamaged and remains in the nominal condition. The interval (22) can be applied to determine one of the basic RUL parameters, i.e., time-to-failure (TTF). The TTF represents the time of the system transition from nominal m_k to damaged state $\bar{m}$ according to the actual degradation process. The knowledge about the interval (22) allows dividing it into n classes. Each of these classes represents a different condition of the bearing degradation level. In practice, it can be assumed with a high probability that such classes can be uniformly distributed over (22) with a spread of

$$z_j = \underline{m} + (j-1)\frac{\bar{m}-\underline{m}}{n-1}, \quad j=1,\dots,n. \tag{23}$$

This assumption can be justified by the fact that, in general, the degradation signal z_k evolves within (22). Thus, the degradation signal of each component being monitored goes from the minimum up to the maximum bound.

Thus, the classes defined in this way will form a basis for defining membership functions (Zadeh, 1992), which will be used for modeling the unknown structure of the degradation model mimicking the degradation signal z_k. This process will be repeated for a set of various bearings of the same type, which allows designing a degradation database, which can be suitably adapted to the bearing being currently monitored. This means that the closest (in the sense of the degradation profile) fuzzy logic model will be used to get a prediction of the future degradation z_k.

In the literature on fuzzy logic, various types of membership functions can be found, among others sigmoidal, trapezoidal, piecewise linear, Gaussian or singleton (Zadeh, 1992). In this paper, it is assumed that the triangular membership functions will be applied (cf. Fig. 3):

$$\begin{aligned} &a_j = b_{j-1}, \quad b_j = z_j, \\ &c_j = b_{j+1}, \quad j=2,\dots,n-1, \\ &a_1 = b_1, \qquad c_n = b_n, \end{aligned} \tag{24}$$

where parameters a_j, b_j, c_j describe the j-th membership function.

On the basis of the assumed membership functions, the model of the bearing degradation process can be represented in the form of a Takagi–Sugeno (Tanaka and Sugeno, 1992) model which consists of several submodels

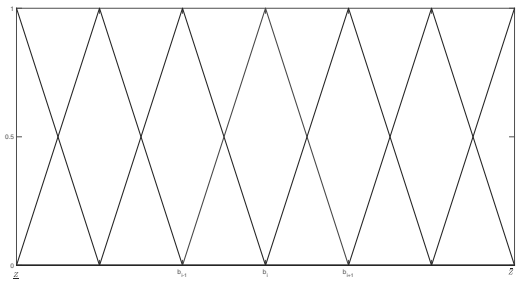

Fig. 3. Triangular membership functions and their application for degradation modeling.

given by

$$\text{IF } m_k \in D_{m,j} \text{ THEN } z_k = r_k^T p^j + v_k, \quad j = 1, \ldots, n. \tag{25}$$

where $D_{m,j}$ represents the fuzzy set described by the j-th triangular membership function (24) and v_k is measurement and modeling uncertainty.

Now, (25) can be rewritten as follows:

$$m_k = \sum_{j=1}^{n} \mu_j(m_k) \left(r_k^T p^j + v_k \right), \tag{26}$$

$$\sum_{j=1}^{n} \mu_j(m_k) = 1, \quad \mu_j(m_k) \geq 0,$$

where $\mu_j(m_k)$ $(j = 1, \ldots, n)$ stands for the normalized j-th rule firing strength calculated according to the triangular shape (24). Alternatively, the system (26) can be redefined as

$$m_k = \bar{r}_k^T \bar{p} + v_k, \tag{27}$$

where

$$\bar{r} = [\mu_1(m_k) r_k^T, \mu_2(m_k) r_k^T, \ldots, \mu_n(m_k) r_k^T]^T, \tag{28}$$

and

$$\bar{p} = [(p^1)^T, \ldots, (p^n)^T]^T. \tag{29}$$

As can be seen, the quantity m_k in (27) is influenced not only by $\bar{r}$, but also by $2n$ parameters within $\bar{p} \in \mathbb{R}^{2n}$.

It is worth emphasizing that in most cases the number of degradation classes n is relatively low. However, even if the number n is large, it can observed that some of $\mu_l(m_k)$ can be inactive, which means they are equal to zero, until the bearing degradation process enters a given class. The situation described above means that some elements of vector $\bar{r}$ can be constantly equal to zero and this can make the process of parameter estimation more difficult. To solve this problem, the natural properties of triangular membership functions can be used. As can be seen in Fig. 3, for any variable x_k at most two membership functions are active at the same time. In this case Eqn. (26) transforms to the following form:

$$m_k = \mu_j(m_k) r_k^T p^j + \mu_{j+1}(m_k) r_k^T p^{j+1} + v_k, \tag{30}$$

$$\mu_i(m_k) + \mu_{j+1}(m_k) = 1,$$

where $\mu_i(m_k) \geq 0$ for $j = 1, \ldots, n-1$.

Now, assume that v_k can be modeled via the Brownian motion (Gebraeel *et al.*, 2005; Li *et al.*, 2015) and

$$|v_k| \leq \bar{v}, \tag{31}$$

where $\bar{v}$ represents a known upper bound of v_k, which denotes a maximum possible difference between the bearings degradation process (30) and model output $m_{d,k}$,

$$m_{d,k} = \mu_j(z_k) r_k^T p^j + \mu_{j+1}(m_k) r_k^T p^{j+1}, \tag{32}$$
$$\mu_j(m_k) + \mu_{j+1}(m_k) = 1,$$

where $\mu_j(m_k) \geq 0$ and $j = 1, \ldots, n-1$.

The developed methodology for modeling the bearing degradation process on the basis of the historical *run-to-failure* data allows representing it in form of set $l = 1, \ldots, n_h$ models

$$m_{d,k} = \mu_j(m_k) r_k^T p_l^j + \mu_{j+1}(m_k) r_k^T p_l^{j+1}, \tag{33}$$
$$\mu_j(m_k) + \mu_{j+1}(m_k) = 1,$$

where $\mu_j(d_k) \geq 0$ and $j = 1, \ldots, n-1$. The main advantage of such a representation is that instead of processing a large data set, the degradation parameter vector $\bar{p}_l = [(p_l^1)^T, \ldots, (p_l^n)^T]^T$ is only processed.

5.2. Parameter estimation of the fuzzy logic model. A mathematical description of the fuzzy-logic model was presented above. This section presents an algorithm that enables the estimation of $\bar{p}_l$ parameters of this model.

In order to solve this problem, multiple methods of parameter estimation available in the literature can be used. Among the available methods, one of the classes of algorithms, called bounded error, deserves special attention (Arablouei and Doğançay, 2013; Kraus *et al.*, 2007). An advantage of these methods is the possibility of obtaining optimal parameter estimates without knowing the disturbance characteristics. Due to its properties, the Modified quasi-Outer Bounding Ellipsoid (MOBE) algorithm (Arablouei and Doğançay, 2013) algorithm deserves special attention. This algorithm is characterized by low computational complexity comparable to the recursive least-squares (RLS) algorithm.

At the beginning it should be mentioned that in order to simplify the notation, the index l (denoting

the l-th bearing) has been omitted. The algorithm for estimating the parameters of the developed fuzzy logic model has the form of Algorithm 2. Finally, note that the adaptation of the MOBE algorithm is not accidental and it has a strong scientific background (Arablouei and Doğançay, 2013) motivated by the fact that it copes better with the situations in which the degradation signal is more or less on a constant level. In such cases, the lack of suitable persistent excitation (Witczak, 2014) may lead to numerical problems with the application of the RLS algorithm. Indeed, as can be observed in Algorithm 2, new data contribute to the parameter estimation iff the current error of the models e_k^j exceeds a given threshold $\bar{v} > 0$. Moreover, λ_k^j plays a role of an adaptive forgetting factor, which overcomes the RLS-based strategies with a constant one (usually within $\lambda \in [0.9, 1]$).

From the analysis of Algorithm 2 it can be seen that it does not update the parameters w_k^j when the absolute value of the current estimation error is lower than $\bar{v}$.

5.3. Modeling of the bearing degradation processes. It should be emphasized that modeling the bearing degradation process should start at the moment of the incipient fault detection in the bearing. Thus, at the beginning, the so-called first prediction time (FPT) t_{FPT} should be defined, which enables the determination of the moment in which the modeling of the process of predicting the remaining useful life of the bearing begins. Among the numerous parameters and signals used in the diagnostic processes of bearings, kurtosis and the root mean square (RMS) deserve special attention. These parameters enable an effective detection of the deteriorating condition of the bearings. It should be underlined that the kurtosis is sensitive to incipient faults (Witczak, 2014) but not best suited to reflect the time varying nature of the degradation process (Gebraeel *et al.*, 2005; Li *et al.*, 2015). The RMS method does not have this weakness and together with the kurtosis (Gebraeel *et al.*, 2005) enables the delivery of clear diagnostic information. Finally, the resulting strategy is given by Algorithm 3. The diagram in Fig. 4 shows the algorithm that allows determining t_{FPT} with application of the kurtosis and then obtaining a model representing the bearing degradation process with the associated parameter updates.

It should be emphasized that as a result of the application of Algorithm 3 (cf. Fig. 4), a set of models corresponding to the run-to-failure of n_h bearings will be obtained. Such models are represented in the set of $n_h \times 2 \times n$ parameters.

Algorithm 2. Fuzzy logic models parameters estimation.

S_0 : Set $k = 1$, set $p_0^i = 0$, $i = 1, \ldots, n$ and $P_0^j = \rho \mathbf{I}$, $j = 1, \ldots, n-1$, where $\rho > 0$ is a large positive constant.

S_1 : Determine a list of active sub-models

$$j = \{i : \mu_i(m_k) + \mu_{j+1}(m_k) = 1, \quad i = 1, \ldots, n-1\}. \tag{34}$$

S_2 : Form temporary regressor and parameter vectors:

$$r_k^j = [\mu_j(m_k) r_k^T, \mu_{j+1}(m_k) r_k^T]^T, \tag{35}$$

$$w_k^j = [(p_k^i)^T, (p_k^{j+1})^T]^T. \tag{36}$$

S_3 : Calculate

$$e_k^j = m_k - (r_k^j)^T w_{k-1}^i. \tag{37}$$

S_4 : If $|e_k^j| > \bar{v}$ then

$$h_k^j = (r_k^j)^T P_{k-1}^j r_k^j, \tag{38}$$

$$\lambda_k^j = \frac{g_k^j}{\frac{|e_k^j|}{\bar{v}} - 1}, \tag{39}$$

$$P_k^j = (\lambda_k^j)^{-1} \left(P_{k-1}^j - P_{k-1}^j r_k^j (r_k^j)^T P_{k-1}^j (g_k^j)^{-1} \right), \tag{40}$$

$$w_k^j = w_{k-1}^j + P_k^j r_k^j e_k^j; \tag{41}$$

otherwise,

$$P_k^j = P_{k-1}^j, \tag{42}$$

$$w_k^j = w_{k-1}^j. \tag{43}$$

S_5 : Set $k = k + 1$ and go to Step 1.

6. Remaining useful life prediction

On the basis of the results obtained in Section 5, it is possible to design the method of the remaining useful life prediction of a currently operating bearing. In the proposed method, which is an extension of the method presented in Fig. 4, an additional task concerning remaining useful life prediction is included. As a result of the introduced changes, Algorithm 4 is proposed. It should be emphasized that during Step 5 the following activities are performed:

1. The current degradation class i is determined in Step 1.

Algorithm 3. Calculation of the t_{FPT} with application of the kurtosis.

S_1 : Compute the average kurtosis μ_K and the standard deviation σ_K for a set of historical data achieved from nominal bearings.

S_2 : Use the $3\sigma_K$ rule to obtain the kurtosis uncertainty interval:

$$\mathbb{K} = [\mu_K - 3\sigma_K, \mu_K + 3\sigma_K]. \tag{44}$$

S_3 : Calculate kurtosis m_f on the basis of the current measurement, where f is a sample number for the current time t_f.

S_4 : Validate m_f on the window $m_f, \ldots, m_{f+n_w}$, i.e., the first element m_{f+j}, $j = 0, \ldots, n_w$ for which the remaining ones are $m_{f+j} \notin \mathbb{K}$, is assumed as the one corresponding to FPT and $t_{\text{FPT}} = t_j$.

S_5 : If t_{FPT} is obtained then the process of bearing degradation modeling is initialized.

2. A set of n_h historical models for class i is obtained:

$$m_{n,k} = \mu_i(m_k) r_k^T p_l^i + \mu_{i+1}(m_k) r_k^T p_l^{i+1}, \quad \mu_i(m_k) + \mu_{i+1}(m_k) = 1. \tag{58}$$

where $\mu_i(m_k) \geq 0, l = 1, \ldots, n_h$.

Based on these results, the following relation between the current and historical models (58) can be defined:

$$Q_l^i = \left(\mu_i(z_k) r_k^T (p_l^i - p^i) + \mu_{i+1}(z_k) r_k^T (p_l^{i+1} - p^{i+1})\right)^2, \tag{59}$$

for $l = 1, \ldots, n_h$ whereby (55) gives the l-th historical model in the i-th degradation class, which is the closest to the currently operating one.

The knowledge of the l-th historical model allows proceeding to Step 6. As was mentioned in Section 5.1, the maximum degradation signal bound by the relation (22) denotes the failure threshold. At this time moment, which signifies the moment of failure, the l-th model should satisfy

$$\bar{m} = \mu_j(\bar{m}) r_f^T p_l^j + \mu_{j+1}(\bar{m}) r_f^T p_l^{j+1}, \quad \mu_j(\bar{m}) + \mu_{j+1}(\bar{m}) = 1, \quad \mu_j(\bar{m}) \geq 0. \tag{60}$$

for some $i \leq j \leq n-1$ and $f > k$.

By analyzing the relationship (23), it can be deduced that $j = n - 1$. Furthermore, from Fig. 3, it can be seen that $\mu_{n-1}(\bar{m}) = 0$ and $\mu_n(\bar{m}) = 1$. In such a case, the

Algorithm 4. Time-to-failure calculation.

S_0 : Set $k = 1$, set $p_0^i = 0$, $i = 1, \ldots, n$ and $P_0^i = \rho \mathbf{I}$, $j = 1, \ldots, n-1$, where $\rho > 0$ is a large positive constant.

S_1 : Form the set of currently active sub-models:

$$j = \{i : \mu_j(m_k) + \mu_{i+1}(m_k) = 1, \; i = 1, \ldots, n-1\}. \tag{45}$$

S_2 : Set regressor and parameter vectors:

$$r_k^j = [\mu_j(m_k) r_k^T, \mu_{j+1}(m_k) r_k^T]^T, \tag{46}$$

$$w_k^j = [(p_k^j)^T, (p_k^{j+1})^T]^T. \tag{47}$$

S_3 : Calculate

$$e_k^j = m_k - (r_k^j)^T w_{k-1}^j. \tag{48}$$

S_4 : If $|e_k^i| > \bar{v}$ then

$$h_k^j = (r_k^j)^T P_k^j r_k^j, \tag{49}$$

$$\lambda_k^j = \frac{g_k^j}{\frac{|e_k^j|}{\bar{v}} - 1}, \tag{50}$$

$$P_k^i = (\lambda_k^j)^{-1} \left(P_{k-1}^j - P_{k-1}^j r_k^j (r_k^j)^T P_{k-1}^j (g_k^j)^{-1}\right), \tag{51}$$

$$w_k^j = w_{k-1}^j + P_k^j r_k^i e_k^j; \tag{52}$$

otherwise,

$$P_k^j = P_{k-1}^j, \tag{53}$$

$$w_k^j = w_{k-1}^j. \tag{54}$$

S_5 : Find the closest historical model

$$l = \arg \min_{l=1,\ldots,n_h} Q_l^j. \tag{55}$$

S_6 : Predict t_f:

$$f = \frac{\bar{m} - p_{1,l}^n}{T_s p_{2,l}^n}, \quad t_f = T_s \times f. \tag{56}$$

S_7 : Calculate RUL

$$\text{RUL}_k = (f - k) T_s. \tag{57}$$

S_8 : Set $k = k + 1$ and go to Step 1.

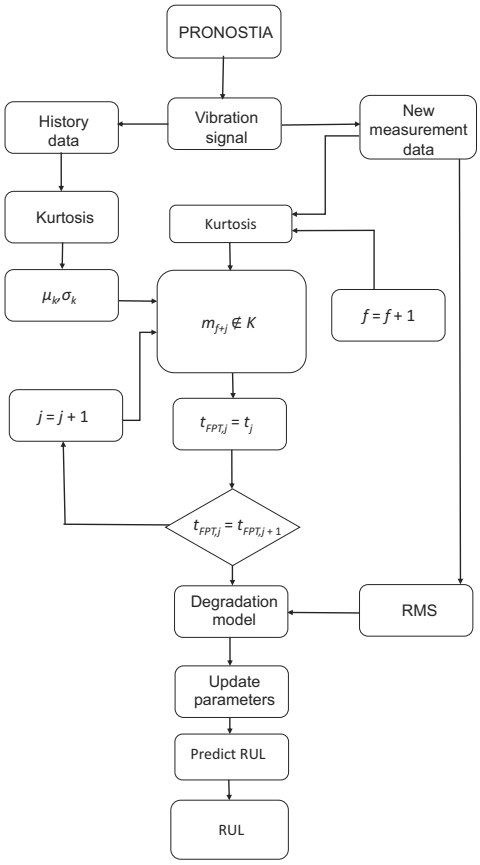

Fig. 4. Flowchart of the proposed framework.

remaining task is to calculate $f > k$ for which (60) is fulfilled, i.e.,

$$\bar{m} = r_f^T p_l^n. \tag{61}$$

This problem in solved on the basis of (21) for the regressor $r_f = [1, t_f]^T$ with $t_f = T_s \times f$, where T_s stands for the known sampling time. Thus, (61) represents the failure time defined by relation (56).

Finally, it should be noted that the above algorithm should be applied for all wheel loaders. This means that t_f (see (56)) for the i-th wheel loader is simply denoted by $\bar{t}_i$ (cf. (11)).

7. H-A FTC of multiple wheel loaders

The structure of the loading system and its operating procedure described in Section 2 allows scheduling the work of n_v wheel loaders according to (16). The optimization problem of each loading tasks k (see (16)) is calculated with the use of an external application and the results of optimization are delivered by the dedicated platform to KIS.ME. As a result, commands provided by the human operator are replaced by the platform ones.

Let us start with recalling that Algorithm 2 provides the actual transportation times of the i-th transporter, i.e., $c_i(k)^m$ and $b_i(k)^m$. Thus, by comparing them with the nominal values $c_i(k)$ and $b_i(k)$ (cf. (5) and (6)) one can estimate transportation faults, which are simply defined as delays

$$\begin{aligned} &\text{IF } c_i(k)^m \leq c_i(k) \text{ THEN } f_{i,c}(k) = 0 \\ &\text{ELSE } f_{i,c}(k) = c_i(k)^m - c_i(k) \end{aligned} \tag{62}$$

and

$$\begin{aligned} &\text{IF } b_i(k)^m \leq b_i(k) \text{ THEN } f_{i,b}(k) = 0 \\ &\text{ELSE } f_{i,b}(k) = b_i(k)^m - b_i(k). \end{aligned} \tag{63}$$

Note that this representation corespondents to delays of $c_i(k)$ and $b_i(k)$, respectively. Finally, the combination of all developed methods, including the system degradation modeling and RUL prediction methods, enables determination of fault estimates. On the basis of this knowledge, it is possible to design the H-A FTC system for a group of wheel loaders, taking into account the degradation state of their bearings. The fault-tolerant control part of the proposed strategy is adapted from our previous works (Witczak *et al.*, 2020b; 2020c). It is modified by exchanging the original cost function (Witczak *et al.*, 2020c), with (12), denoted by J, which covers

- J_u: performance,
- J_α: fault-tolerance,
- J_H: health-awareness.

All these factors are merged together with a suitable relevance weights γ_1, γ_2, γ_3, which express their relative importance. The detailed mechanism of the developed scheme is given by Algorithm 5.

8. Assessment of the effectiveness of the developed H-A FTC method

The main objective of this section is to provide an experimental verification of the proposed approach. This approach is based on Algorithms 2–5. This section is divided into two subsections. The first one presents the results of remaining useful life predictions during run-to-failure tests. The results obtained from this subsection provide information about the remaining useful life models. This enables the correct application of the second part of the framework. The second subsection confirms the correctness of the health-aware fault-tolerant control of the wheel loaders fleet according to the time-to-failure measure from the first part of the section.

Algorithm 5. H-A FTC of multiple wheel loaders.

S_0 : Set: $k = 1$, $v(0)$, and N_p, u_E.

S_1 : Form: $\mathbb{N}(k), \ldots, \mathbb{N}(k + N_E)$.

S_2 : For the i-th wheel loaders carrying the $(k-1)$-th load of rock aggregate assume $v_i(k-1) = e$ and then obtain $b_i(k-1)^m$, $c_i^m(k-1)$ and $z(k-1)$.

S_3 : Perform fault estimation with (62) and set $\hat{f}_{i,b} = f_{i,b}(k-1)$ and $\hat{f}_{i,c} = f_{i,c}(k-1)$.

S_4 : If $\hat{f}_{i,b} \neq 0$ and/or $\hat{f}_{i,b} \neq 0$, calculate elements of control matrix $A(\cdot,\cdot,\cdot)$ in (15), relating to z_i of the i-th wheel loaders:

$$\begin{aligned} A_{v,i,i}(\cdot,\cdot,\cdot)_{i,i} &= b_i(k-1) + c_i(k-1) \\ &\quad + \hat{f}_{i,b} + \hat{f}_{i,c}, A_{v,n_v+1,i}(\cdot,\cdot,\cdot) \\ &= b_i(k-1) + c_i(k-1) \\ &\quad + c_i(k) + \hat{f}_{i,b} + \hat{f}_{i,c} + \hat{f}_{i,c} + v_i(k), \end{aligned} \tag{64}$$

and

$$b_i(k) = \max\left(e, b(k) + \hat{f}_{i,b} + v_i(k)\right), \tag{65}$$

$$c_i(k) = \max\left(e, c(k) + \hat{f}_{i,c} + v_i(k)\right). \tag{66}$$

If $\hat{f}_{i,b} \neq 0$, then set

$$B_{v,n_v+1}(\cdot,\cdot) = b_v(k) \tag{67}$$

while

$$\begin{aligned} b_v(k) = \max(&c_1(k) + v_1(k), \ldots, c_{n_v}(k) \\ &+ v_{n_v}(k)). \end{aligned} \tag{68}$$

S_5 : Using Algorithm 5, Calculate $\bar{t}_i$ for each wheel loader.

S_6 : Determine $\tilde{v}(k)^*$, $\tilde{u}(k)^*$, $\tilde{\alpha}(k)$ by (17) for constraints (3)–(7).

S_7 : Assume $u(k)^*$ and $v(k)^*$ in the system consisting of all wheel loaders.

S_8 : Set $k = k + 1$ and go to Step 1.

8.1. RUL prediction of ball bearings. The data obtained thanks to the PRONOSTIA test platform (Nectoux *et al.*, 2012) made it possible to validate the developed RUL prediction method. The considered data come from accelerated tests and are intended only to verify the prepared software. The test

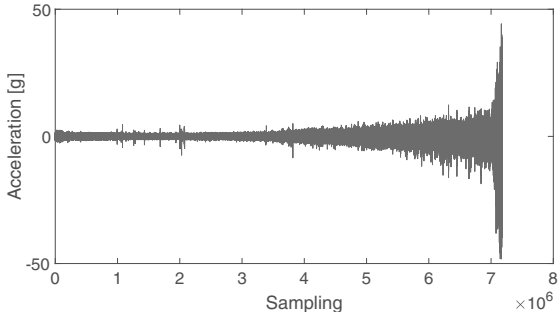

Fig. 5. Raw vibration signal of ball bearing.

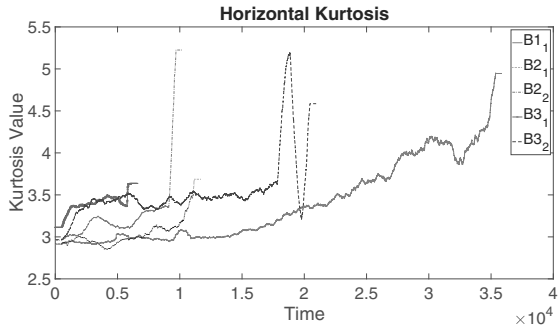

Fig. 6. Kurtosis of vibration signals.

bearings were evaluated from 6 to 8 hours. While the actual operating time of the bearings is usually measured in months. The prepared solution enables the correct modeling of the bearing vibration signal. The increase in the bearing vibration is due to the degradation of the internal bearing surfaces (see Fig. 5). In the same way, a diagnostic method has been proposed by Yan and Gao (2009) where three accelerometers were used to measure the vibration on the tested bearings.

The difference with respect to the above applications is that in this one a load is applied to the bearing to accelerate its degradation. In the particular case of bearing test beds, and compared to those proposed in the literature, the data provided by the PRONOSTIA experimental platform are different in the sense that they correspond to "normally" degraded bearings. This means that the defects were not initially initiated on the bearings and that each degraded bearing contains almost all the types of defects (balls, rings and cage). The acquired experimental data can then be used for fault detection, diagnosis and forecast.

Figure 6 shows the vibration kurtosis signal, which is necessary to estimate the historical models. The value 3 pertains to the healthy state of a ball bearing. However, a value greater than 4 indicates end-of-life, and the ball bearing should be replaced. To normalize the data, a kurtosis shift was performed. The zero

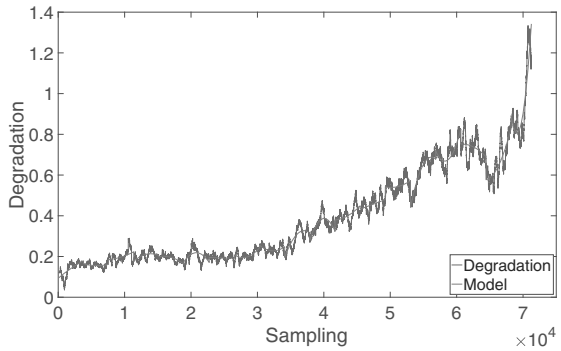

Fig. 7. Learning process.

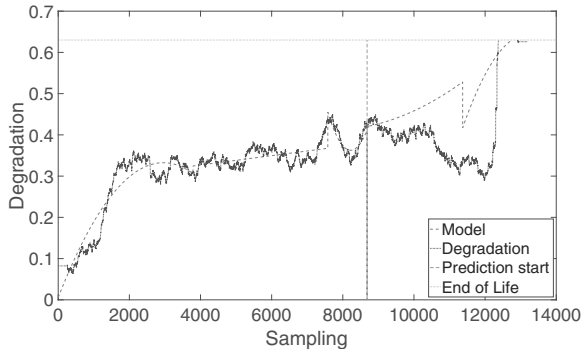

Fig. 8. Prediction of RUL.

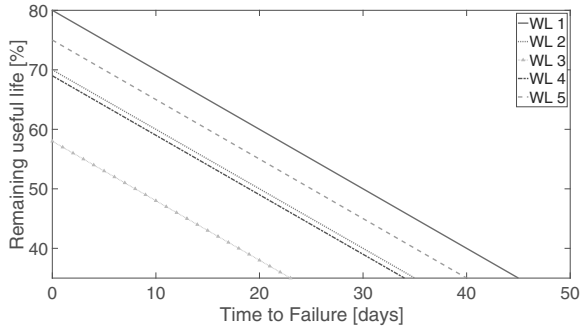

Fig. 9. Time to failure of wheel loaders.

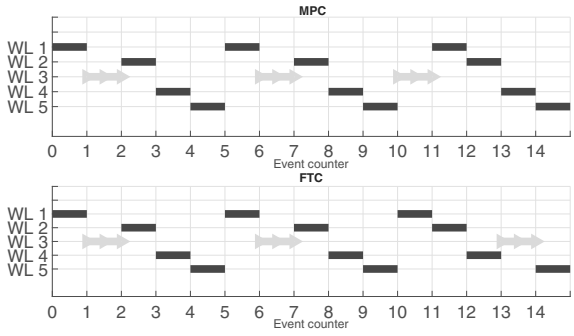

Fig. 10. Scheduling scheme for the fault-free scenario.

level indicates the healthy condition and a value greater than 1 indicates permanent bearing damage. Finally, the historical models were prepared to serve as benchmarks for future degradation prediction (see Fig. 7), and a simulation of the remaining useful life of one bearing was performed. A sample remaining useful life prediction after 65% of ball bearing life was presented in Fig. 8. This example shows the correctness of the proposed approach. The entire remaining useful life framework enables us to predict the time-to-failure of ball bearings, which can be used in wheel loaders.

8.2. Fleet scheduling. The considered scenario contains five wheel loaders, the scheduling prediction horizon was set to four. Verification was prepared for 15 loading tasks. For that purpose, the sequence of tasks $(B, M, T, G, W, M, M, R, G, B, M, Y, B, M, W)$ is employed. Each letter corresponds to the colors names, which represent the loading mass for each task (see Table 1). The use of this idea enables implementation in multinational companies without the requirement of employee training or language learning. The use of color markings is universal. The results provided by Algorithm 4 enable us to calculate the value of time-to-failure. Figure 9 shows the operation time (in days) of wheel loaders before necessary maintenance. We assume that the decrease in the remaining useful life to the level of 35% corresponds to the necessity of replacing the ball bearings. The discussed figure shows the situation with the equal load on all wheel loaders (WLs). The third WL has the shortest TTF. This means that it cannot be exploited as extensively as other WLs.

Figure 10 shows the transportation events realized by five WLs. The third WL has the lowest condition of ball bearings and was assigned to the easiest (low weight) task. This WL is shown in the form of an irregular shape in the Gantt diagram. The task realization times are shown in Fig. 11. During the current scenario, no faults, i.e., delays, are introduced. Figure 12 confirms the correctness of the proposed approach. Indeed, the third WL was chosen less often than others during 300 loading tasks.

The second scenario corresponds to a situation where the second WL has a fault (delay) and it is described as follows:

Scenario. The wheel loader fault is

$$f_{2,b}(k) = \begin{cases} 0, & k < 7, \\ 4, & \text{otherwise.} \end{cases} \tag{69}$$

A fault of the WL is described as the transportation time

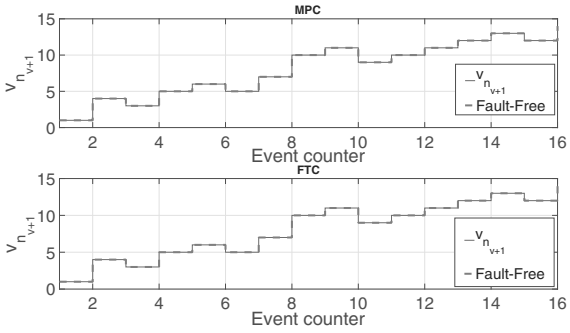

Fig. 11. Times of completed tasks for the fault-free scenario.

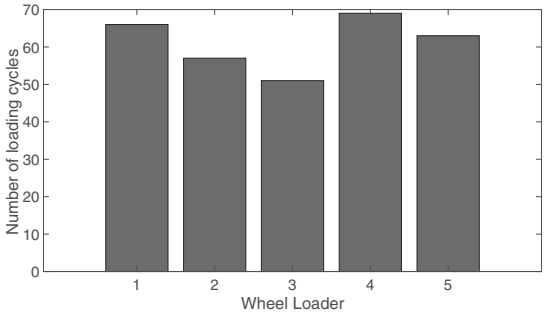

Fig. 12. Usage of wheel loaders during 300 cycles.

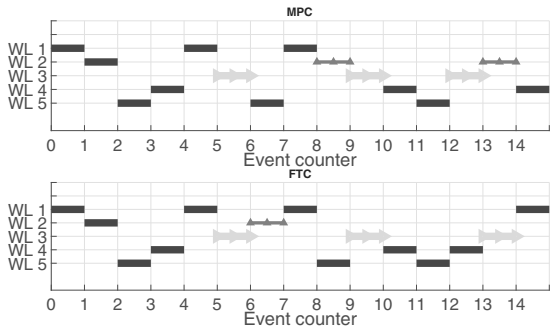

Fig. 13. Scheduling scheme for the scenario of the fault of the 2nd WL.

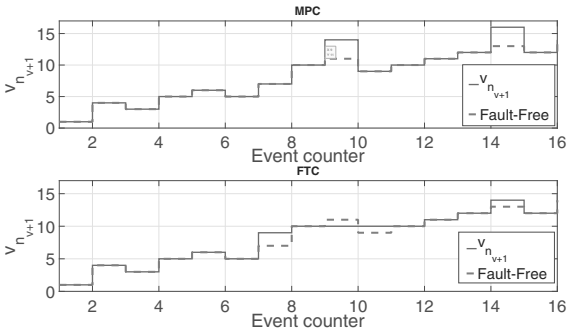

Fig. 14. Times of completed tasks for fault of the 2nd WL scenario.

delay in the considered scenario, and hence, the second and third WLs should be assigned less often than others.

The Gantt diagram (see Fig. 13) shows the scheduling strategy, which depends on the ball bearings condition and the assigned tasks. The third WL has the easiest tasks and the second one after fault recognition has been less time assigned. This makes it possible to extend the operating time of all WLs before the required maintenance.

The task accomplishment times are presented in Fig. 14. Due to delays in loading (caused by a fault), there are delays in the realization of tasks. Compared with the classical model predictive control (Majdzik *et al.*, 2016), the H-A FTC method correctly assigns tasks to optimize the schedule and loading times.

Figure 15 shows the histogram after 300 tasks. The second WL was chosen less frequently than other WLs. These results confirm the correctness of the proposed solution.

9. Concluding remarks

The primary goal of this paper was to develop a new H-A FTC strategy for a group of cooperating wheel loaders. The proposed approach provides the remaining useful life of ball bearings and combines this with fault-tolerant control to schedule tasks of wheel loaders according to a health indicator of currently available wheel loaders. The method is general in nature and if there are data sets of other bearing types, it will also be effective and its effectiveness depends on these data. At the same time, the method is so constructed that it enables the prediction of the remaining service life of other components.

The proposed solution is based on the available historical data. It can be used with other maintenance components, such as batteries or electronic components (e.g., MOSFET transistors). The main determining factor is the ability to collect degradation data of the component. As a result, a health-aware fault-tolerant control algorithm was developed and applied to the loading task scenario, which verifies the correctness of proposed solution. The achieved results confirm the effective scheduling of tasks. The proposed IoT infrastructure of KIS.ME, provided by RAFI GmbH & Co. KG company, makes it possible to easily transmit the necessary information to the wheel loader driver. The presented performance evaluation enables us to apply the proposed approach in a real health-aware scheduling of multiple wheel loaders.

Acknowledgment

The work was supported by the National Science Center, Poland, under the grant UMO-2017/27/B/ST7/00620.

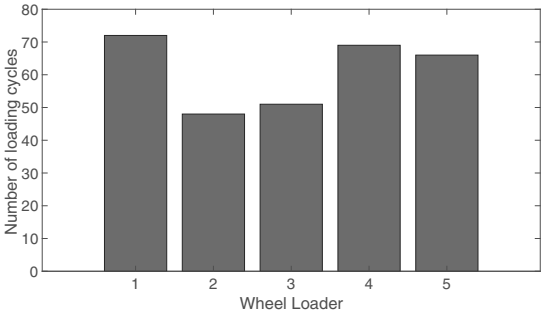

Fig. 15. Usage of wheel loaders during 300 cycles.

References

AlShorman, O., Alkahatni, F., Masadeh, M., Irfan, M., Glowacz, A., Althobiani, F., Kozik, J. and Glowacz, W. (2021). Sounds and acoustic emission-based early fault diagnosis of induction motor: A review study, *Advances in Mechanical Engineering* **13**(2): 1687814021996915.

AlShorman, O., Irfan, M., Saad, N., Zhen, D., Haider, N., Glowacz, A. and AlShorman, A. (2020). A review of artificial intelligence methods for condition monitoring and fault diagnosis of rolling element bearings for induction motor, *Shock and Vibration* **2020**, Article ID: 8843759.

Anis, M.D. (2018). Towards remaining useful life prediction in rotating machine fault prognosis: An exponential degradation model, *Condition Monitoring and Diagnosis (CMD), Bentley, Australia*, pp. 1–6, DOI: 10.1109/CMD.2018.8535765.

Arablouei, R. and Doğançay, K. (2013). Modified quasi-OBE algorithm with improved numerical properties, *Signal Processing* **93**(4): 797–803.

Butkovic, P. (2010). *Max-Linear Systems: Theory and Algorithms*, Springer, London.

Chen, Y., Peng, G., Zhu, Z. and Li, S. (2020). A novel deep learning method based on attention mechanism for bearing remaining useful life prediction, *Applied Soft Computing* **86**: 105–919.

Chudnovsky, B.H. (2012). *Electrical Power Transmission and Distribution*, CRC Press, Boca Raton.

De Schutter, B. and Van Den Boom, T. (2001). Model predictive control for max-plus-linear discrete event systems, *Automatica* **37**(7): 1049–1056.

Do, N.V., Nguyen, H.D. and Selamat, A. (2018). Knowledge-based model of expert systems using Rela-model, *International Journal of Software Engineering and Knowledge Engineering* **28**(08): 1047–1090.

Duan, Z., Wu, T., Guo, S., Shao, T., Malekian, R. and Li, Z. (2018). Development and trend of condition monitoring and fault diagnosis of multi-sensors information fusion for rolling bearings: A review, *International Journal of Advanced Manufacturing Technology* **96**(1): 803–819.

Gao, Z. and Liu, X. (2021). An overview on fault diagnosis, prognosis and resilient control for wind turbine systems, *Processes* **9**(2): 300.

Gebraeel, N., Lawley, M., Li, R. and Ryan, J. (2005). Residual-life distributions from component degradation signals: A Bayesian approach, *IIE Transactions* **37**(6): 543–557.

Hamdi, H., Rodrigues, M., Rabaoui, B. and Benhadj Braiek, N. (2021). A fault estimation and fault-tolerant control based sliding mode observer for LPV descriptor systems with time delay, *International Journal of Applied Mathematics and Computer Science* **31**(2): 247–258, DOI: 10.34768/amcs-2021-0017.

Jain, T. and Yamé, J. (2020). Health-aware fault-tolerant receding horizon control of wind turbines, *Control Engineering Practice* **95**: 104236.

Kraus, T., Mandour, G.I. and Joachim, D. (2007). Estimating the error bound in QOBE vowel classification, *50th Midwest Symposium on Circuits and Systems, Montreal, Canada*, pp. 369–372.

Li, N., Lei, Y., Lin, J. and Ding, S. (2015). An improved exponential model for predicting remaining useful life of rolling element bearings, *IEEE Transactions on Industrial Electronics* **62**(12): 7762–7773.

Li, X., Ding, Q. and Sun, J.-Q. (2018). Remaining useful life estimation in prognostics using deep convolution neural networks, *Reliability Engineering & System Safety* **172**: 1–11.

Lipiec, B., Mrugalski, M. and Witczak, M. (2021). Health-aware fault-tolerant control of multiple cooperating autonoumous vehicles, *IEEE International Conference on Fuzzy Systems (FUZZ-IEEE), Luxembourg, Luxembourg*, pp. 1–7.

Liu, Z. and Zhang, L. (2020). A review of failure modes, condition monitoring and fault diagnosis methods for large-scale wind turbine bearings, *Measurement* **149**: 107002.

Majdzik, P., Akielaszek-Witczak, A., Seybold, L., Stetter, R. and Mrugalska, B. (2016). A fault-tolerant approach to the control of a battery assembly system, *Control Engineering Practice* **55**: 139–148.

Majdzik, P., Witczak, M., Lipiec, B. and Banaszak, Z. (2021). Integrated fault-tolerant control of assembly and automated guided vehicle-based transportation layers, *International Journal of Computer Integrated Manufacturing* **35**(4–5): 1–18.

Mrugalski, M. and Korbicz, J. (2007). Least mean square vs. outer bounding ellipsoid algorithm in confidence estimation of the GMDH neural networks, *in* B. Beliczyński *et al.* (Eds), *Adaptive and Natural Computing Algorithms, Part 2*, Lecture Notes in Computer Science, Vol. 4432, Springer, Berlin, p. 19.

Nath, A.G., Udmale, S.S. and Singh, S.K. (2021). Role of artificial intelligence in rotor fault diagnosis: A comprehensive review, *Artificial Intelligence Review* **54**(4): 2609–2668.

Nectoux, P.R.G., Medjaher, K., Ramasso, E., Morello, B., Zerhouni, N. and Varnier., C. (2012). PRONOSTIA: An experimental platform for bearings accelerated life test, *IEEE International Conference on Prognostics and Health Management, Denver, USA,* pp. 1–8.

Pazera, M., Buciakowski, M., Witczak, M. and Mrugalski, M. (2020). A quadratic boundedness approach to a neural network-based simultaneous estimation of actuator and sensor faults, *Neural Computing & Applications* **32**(2, SI): 379–389.

Salazar, J.C., Sanjuan, A., Nejjari, F. and Sarrate, R. (2020). Health-aware and fault-tolerant control of an octorotor UAV system based on actuator reliability, *International Journal of Applied Mathematics and Computer Science* **30**(1): 47–59, DOI: 10.34768/amcs-2020-0004.

Seybold, L., Witczak, M., Majdzik, P. and Stetter, R. (2015). Towards robust predictive fault-tolerant control for a battery assembly system, *International Journal of Applied Mathematics and Computer Science* **25**(4): 849–862, DOI: 10.1515/amcs-2015-0061.

Singleton, K.R., Strangas, E.G., Cui, H. and Aviyente, S. (2015). Extended Kalman filtering for remaining-useful-life estimation of bearings, *IEEE Transactions on Industrial Electronics* **62**(3): 1781–1790.

Sun, B., Li, Y., Wang, Z., Ren, Y., Feng, Q., Yang, D., Lu, M. and Chen, X. (2019). Remaining useful life prediction of aviation circular electrical connectors using vibration-induced physical model and particle filtering method, *Microelectronics Reliability* **92**: 114–122.

Sutrisno, E., Oh, H. and Vasan, A.S.S. (2012). Estimation of remaining useful life of ball bearings using data driven methodologies, *IEEE Conference on Prognostics and Health Management (PHM), Denver, USA*, pp. 1–7.

Tanaka, K. and Sugeno, M. (1992). Stability analysis and design of fuzzy control systems, *Fuzzy Sets and Systems* **45**(2): 135–156.

Van Den Boom, T. and De Schutter, B. (2006). Modelling and control of discrete event systems using switching max-plus-linear systems, *Control Engineering Practice* **14**(10): 1199–1211.

Wang, C., Lu, N., Wang, S., Cheng, Y. and Jiang, B. (2018). Dynamic long short-term memory neural-network-based indirect remaining-useful-life prognosis for satellite lithium-ion battery, *Applied Sciences* **8**(11): 2078.

Wei, Y., Li, Y., Xu, M. and Huang, W. (2019). A review of early fault diagnosis approaches and their applications in rotating machinery, *Entropy* **21**(4): 409, DOI: 10.3390/e21040409.

Witczak, M. (2014). *Fault Diagnosis and Fault-Tolerant Control Strategies for Non-Linear Systems*, Springer, Heidelberg.

Witczak, M., Lipiec, B., Mrugalski, M., Seybold, L. and Banaszak, Z. (2020a). Fuzzy modelling and robust fault-tolerant scheduling of cooperating forklifts, *IEEE International Conference on Fuzzy Systems (FUZZ-IEEE), Glasgow, UK*, pp. 1–10.

Witczak, M., Majdzik, P., Stetter, R. and Lipiec, B. (2020b). A fault-tolerant control strategy for multiple automated guided vehicles, *Journal of Manufacturing Systems* **55**: 56–68.

Witczak, M., Mrugalski, M., Pazera, M. and Kukurowski, N. (2020c). Fault diagnosis of an automated guided vehicle with torque and motion forces estimation: A case study, *ISA Transactions* **104**: 370–381.

Xie, X., Ma, D., Yue, D. and Xia, J. (2021). Gain-scheduling fault estimation for discrete-time Takagi–Sugeno fuzzy systems: A depth partitioning approach, *IEEE Transactions on Circuits and Systems I: Regular Papers* **69**(4): 1693–1703.

Yan, R. and Gao, R.X. (2009). Multi-scale enveloping spectrogram for vibration analysis in bearing defect diagnosis, *Tribology International* **42**(2): 293–302.

Zadeh, L.A. (1992). Knowledge representation in fuzzy logic, *in* R.R.Yager and L.A. Zadeh (Eds), *An Introduction to Fuzzy Logic Applications in Intelligent Systems*, Springer, Boston, pp. 1–25.

Zhang, L., Mu, Z. and Sun, C. (2018). Remaining useful life prediction for lithium-ion batteries based on exponential model and particle filter, *IEEE Access* **6**: 17729–17740.

Zhou, Y., Huang, Y., Pang, J. and Wang, K. (2019). Remaining useful life prediction for supercapacitor based on long short-term memory neural network, *Journal of Power Sources* **440**: 227149.

Bogdan Lipiec was born in Poland in 1994. He received his MSc degree in automatic control and robotics from the University of Zielona Góra, Poland, in 2018. He also holds a BSc degree in automation from Technische Hochschule Mittelhessen, Germany (2016). His current research interests include remaining useful life prediction, computational intelligence, and fault-tolerant control (FTC). He has published 14 papers in international journals, book chapters, and conference proceedings. Since 2021, Bogdan Lipiec has been a lecturer at the Institute of Control and Computation Engineering, University of Zielona Góra.

Marcin Mrugalski was born in Poland in 1975. He received his MSc and PhD degrees in electrical engineering from the University of Zielona Góra, Poland, in 1999 and 2004, respectively. He obtained his DSc degree in computer science from the Częstochowa University of Technology in 2014. He has been an associate professor of computer science at the Institute of Control and Computation Engineering, University of Zielona Góra, since 2014. His current research interests include neural networks, computational intelligence, fault diagnosis and fault tolerant control. He has published one monograph and more than 70 papers in international journals, book chapters and conference proceedings.

Marcin Witczak was born in Poland in 1973, received his MSc degree in electrical engineering from the University of Zielona Góra (Poland), his PhD degree in automatic control and robotics from the Wrocław University of Technology (Poland), and his DSc degree in electrical engineering from the University of Zielona Góra, in 1998, 2002 and 2007, respectively. In 2015 he received a full professorial title. Since then, Marcin Witczak has been a professor of automatic control and robotics at the Institute of Control and Computation Engineering, University of Zielona Góra. His current research interests include computational intelligence, fault detection and isolation (FDI), fault-tolerant control (FTC), as well as experimental design and control theory. Marcin Witczak has published more than 200 papers in international journals and conference proceedings. He is an author of four monographs and 30 book chapters. Since 2015, he has been a member of the Committee on Automatic Control and Robotics of the Polish Academy of Sciences. As of 2018, he is also an associated editor of *ISA Transactions*.

Ralf Stetter holds a PhD degree in mechanical engineering from the Technical University of Munich, Germany. He had worked as a product development engineer and a team leader at Audi AG, Ingolstadt, Germany. In 2004 he was appointed a professor of design and development at the Ravensburg–Weingarten University of Applied Sciences (RWU). Since 2006 he has also been a project leader at the Steinbeis Transfer Center for Automotive Systems.

Received: 5 January 2022
Revised: 29 May 2022
Re-revised: 15 June 2022
Accepted: 30 June 2022